Atmospheric
Chemistry
and Physics

Mitigation of PM$_{2.5}$ and ozone pollution in Delhi: a sensitivity study during the pre-monsoon period

Ying Chen[1,2], Oliver Wild[1,2], Edmund Ryan[1,9], Saroj Kumar Sahu[4], Douglas Lowe[5], Scott Archer-Nicholls[6], Yu Wang[5], Gordon McFiggans[5], Tabish Ansari[1], Vikas Singh[7], Ranjeet S. Sokhi[8], Alex Archibald[6], and Gufran Beig[3]

[1]Lancaster Environment Centre, Lancaster University, Lancaster, LA1 4YQ, UK
[2]Data Science Institute, Lancaster University, Lancaster, LA1 4YW, UK
[3]Indian Institute of Tropical Meteorology, Pune, India
[4]Environmental Science, Department of Botany, Utkal University, Bhubaneswar, India
[5]Centre for Atmospheric Sciences, School of Earth, Atmospheric and Environmental Sciences,
University of Manchester, Manchester, M13 9PL, UK
[6]NCAS Climate, Department of Chemistry, University of Cambridge, Cambridge, CB2 1EW, UK
[7]National Atmospheric Research Laboratory, Gadanki, Andhra Pradesh, India
[8]Centre for Atmospheric and Climate Physics Research, University of Hertfordshire, Hatfield, Hertfordshire, UK
[9]Department of Mathematics, University of Manchester, Manchester, M13 9PL, UK

Correspondence: Ying Chen (y.chen65@lancaster.ac.uk)

Abstract. Fine particulate matter (PM$_{2.5}$) and surface ozone (O$_3$) are major air pollutants in megacities such as Delhi, but the design of suitable mitigation strategies is challenging. Some strategies for reducing PM$_{2.5}$ may have the notable side effect of increasing O$_3$. Here, we demonstrate a numerical framework for investigating the impacts of mitigation strategies on both PM$_{2.5}$ and O$_3$ in Delhi. We use Gaussian process emulation to generate a computationally efficient surrogate for a regional air quality model (WRF-Chem). This allows us to perform global sensitivity analysis to identify the major sources of air pollution and to generate emission-sector-based pollutant response surfaces to inform mitigation policy development. Based on more than 100 000 emulation runs during the pre-monsoon period (peak O$_3$ season), our global sensitivity analysis shows that local traffic emissions from the Delhi city region and regional transport of pollution emitted from the National Capital Region (NCR) surrounding Delhi are dominant factors influencing PM$_{2.5}$ and O$_3$ in Delhi. They together govern the O$_3$ peak and PM$_{2.5}$ concentration during daytime. Regional transport contributes about 80% of the PM$_{2.5}$ variation during the night. Reducing traffic emissions in Delhi alone (e.g. by 50%) would reduce PM$_{2.5}$ by 15 %–20 % but lead to a 20 %–25 % increase in O$_3$. However, we show that reducing NCR regional emissions by 25 %–30 % at the same time would further reduce PM$_{2.5}$ by 5 %–10 % in Delhi and avoid the O$_3$ increase. This study provides scientific evidence to support the need for joint coordination of controls on local and regional scales to achieve effective reduction in PM$_{2.5}$ whilst minimising the risk of O$_3$ increase in Delhi.

1 Introduction

Exposure to air pollutants increases morbidity and mortality (J. Huang et al., 2018; WHO, 2013). The urban air quality in India, especially in Delhi, is currently among the poorest in the world (WHO, 2013, 2016a, b). In addition to the local impacts, the Indian monsoon can transport air pollutants to remote oceanic regions, inject them into the stratosphere and redistribute them globally (Lelieveld et al., 2018). This makes the impact of Indian air pollution wide-ranging regionally and globally, and it has interactions with climate and ecosystems worldwide (Menon et al., 2002; Gao et al., 2019).

   PM$_{2.5}$ (particulate matter with an aerodynamic diameter of less than 2.5 µm) is a major air pollutant, causing increases in

disease (Pope et al., 2009; Gao et al., 2015; Stafoggia et al., 2019) and reduced visibility (Mukherjee and Toohey, 2016; Wang and Chen, 2019; Khare et al., 2018). The population of India experiences high PM$_{2.5}$ exposure, and this is responsible for ~ 1 million premature deaths per year (Conibear et al., 2018; Gao et al., 2018). Residential emissions are estimated to contribute $\sim 50\%$ of PM$_{2.5}$ concentrations and to cause more than 0.5 million annual mortalities across India (Conibear et al., 2018). Previous studies reported an annual averaged PM$_{2.5}$ loading of 110–140 µg m^{-3} in Delhi during 2015–2018, leading to $\sim 10\,000$ premature deaths per year in the city (Chen et al., 2019; Chowdhury and Dey, 2016; WHO, 2016a). In Delhi, the traffic sector ($\sim 50\%$) and the domestic sector ($\sim 20\%$) are the major local contributors to PM$_{2.5}$ (Marrapu et al., 2014). Efforts to control traffic emissions in Delhi in recent years by introducing an alternating "odd–even" licence plate policy have led to reductions in PM$_{2.5}$ of less than 10% (Chowdhury et al., 2017). This indicates that there is an urgent need for a coordinated plan to mitigate PM$_{2.5}$ pollution (Chowdhury et al., 2017).

Surface ozone (O$_3$), another major air pollutant, is damaging to health and reduces crop yields (Ashworth et al., 2013; Lu et al., 2018; Kumar et al., 2018). The risks of respiratory and cardiovascular diseases are increased from short-term exposure to high ambient O$_3$ and from long-term exposure at low levels (WHO, 2013; Turner et al., 2016; Fleming et al., 2018). Oxidation of volatile organic compounds (VOCs) in the presence of nitrogen oxides (NO$_x$) is the main source of surface ozone. Rapid economic development in India has greatly increased the emissions of these O$_3$ precursors (Duncan et al., 2016), leading to significant increases in O$_3$ especially during the pre-monsoon period (Ghude et al., 2008). Hourly maximum O$_3$ reaches as much as 140 ppbv during the pre-monsoon season in Delhi (Ghude et al., 2008), comparable to the most polluted regions in China (150 ppbv; Wang et al., 2017) and higher than the most polluted areas in the US (110 ppbv; Lu et al., 2018).

Mitigation of PM$_{2.5}$ pollution may lead to an increase in surface ozone because the dimming effect of aerosols and removal of hydroperoxy radicals are reduced, facilitating O$_3$ production (X. Huang et al., 2018; Li et al., 2018; Hollaway et al., 2019). Furthermore, co-reduction of NO$_x$ and PM$_{2.5}$ emissions may increase O$_3$ in cities where O$_3$ production is in a VOC-limited photochemical regime (Ran et al., 2009; Xing et al., 2017, 2018). This has recently been reported in a number of Asian megacities, e.g. Shanghai (Silver et al., 2018), Beijing (Wu et al., 2015; Liu et al., 2017; Chen et al., 2018) and Guangzhou (Liu et al., 2013). Delhi and coastal cities in India, which are known to be VOC-limited (Sharma et al., 2017), may face increased O$_3$ as a side effect of emission controls focused on PM$_{2.5}$. Therefore, studies of mitigation strategies that target both PM$_{2.5}$ and O$_3$ are urgently needed (Chen et al., 2018), particularly as urban air pollution in India has been much less well studied than in many other countries.

To investigate the impacts of mitigation strategies with respect to both PM$_{2.5}$ and O$_3$, we demonstrate a framework for generating emission-sector-based pollutant response surfaces using Gaussian process emulation (O'Hagan and West, 2009; O'Hagan, 2006). The response surfaces describe how the pollutants, i.e. PM$_{2.5}$ and O$_3$, will respond to the changes in emissions from different sectors. We conduct global sensitivity analysis to identify the dominant emission sectors controlling PM$_{2.5}$ and O$_3$ and then generate sector-based response surfaces to quantify the impacts on PM$_{2.5}$ and O$_3$ of emission reductions. In contrast to simple sensitivity analysis varying one input at a time, this allows full exploration of the entire input space, accounting for the interactions between different inputs (Pisoni et al., 2018; Saltelli et al., 1999). Conventionally, chemical transport models (CTMs) are used to calculate the impacts on pollutants concentrations of different mitigation scenarios. However, the computational expense of CTMs makes them unsuitable for performing global sensitivity analysis or generating response surfaces, which usually require thousands of model runs. To overcome this difficulty, source–receptor relationships (Amann et al., 2011) or computationally efficient surrogate models, trained on a limited number of CTM simulations, are used to replace the expensive CTM. These approaches have been used to perform sensitivity and uncertainty analysis of regional air quality models (Pisoni et al., 2018), assessment of regional air quality plans (Zhao et al., 2017; Xing et al., 2017; Pisoni et al., 2017; Thunis et al., 2016), and sensitivity and uncertainty analysis of global and climate simulations (Ryan et al., 2018; Lee et al., 2012, 2016). Here, we use the surrogate model to explore the sensitivity of PM$_{2.5}$ and O$_3$ to sector-based emission controls in Delhi for developing a mitigation strategy addressing both pollutants.

In this study, we demonstrate the value of such a framework for supporting decision makers in determining better mitigation strategies. We give examples of its use in investigating impacts of mitigation scenarios on PM$_{2.5}$ and O$_3$ pollution in Delhi and demonstrate that regional joint coordination of emission controls over National Capital Region (NCR) of Delhi is essential for an effective reduction of PM$_{2.5}$ whilst minimising the risk of O$_3$ increase.

2 Materials and methods

2.1 WRF-Chem model baseline simulation

WRF-Chem (v3.9.1) – an online, fully coupled chemistry transport model (Grell et al., 2005) – has been widely used in previous studies of air quality across India (Marrapu et al., 2014; Mohan and Gupta, 2018; Gupta and Mohan, 2015; Mohan and Bhati, 2011). The model has also been used to estimate the health burden (Conibear et al., 2018; Ghude et al., 2016) and reduction in crop yields (Ghude et al., 2014) from the exposure to PM$_{2.5}$ and O$_3$ over India.
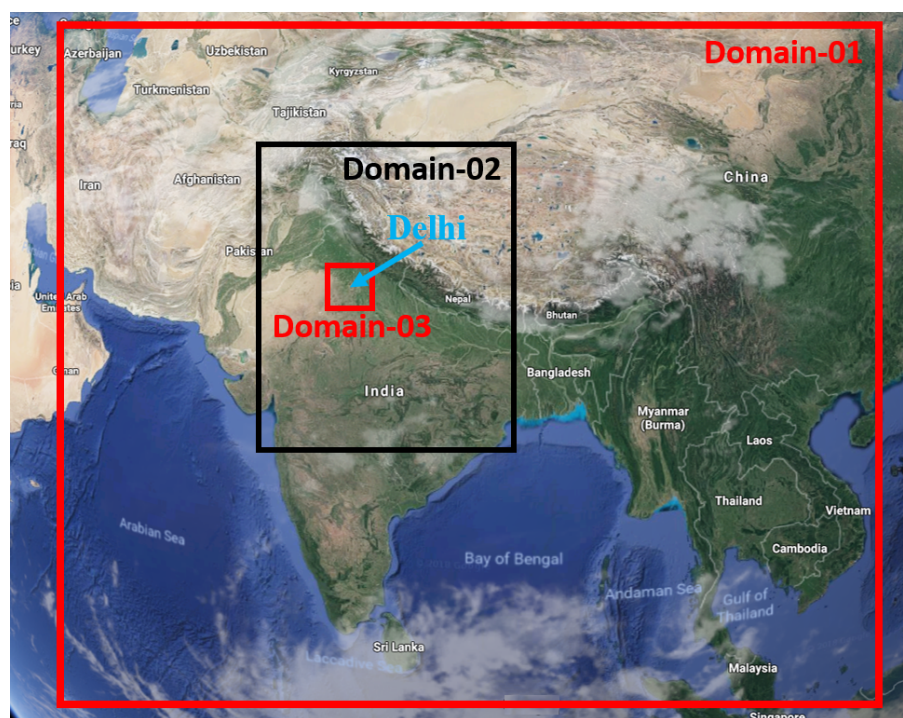
Figure 1. Map of simulation domains, modified from © Google Earth.

In this study, we focus on the hot and dry pre-monsoon period in Delhi, when average temperatures are around 32 °C and relative humidity (RH) is about 35 % (Ojha et al., 2012). O$_3$ approaches its annual peak in the pre-monsoon period due to strong solar radiation (Ghude et al., 2008; Ojha et al., 2012). During the pre-monsoon period, desert dust can contribute significantly to particulate matter in Delhi (Kumar et al., 2014a, b). Here, we perform WRF-Chem simulation for the period of 2–15 May 2015 (with 2 additional days for spin-up), when Delhi was not significantly influenced by dust storms, according to MODIS observations (https://earthdata.nasa.gov/earth-observation-data/near-real-time/hazards-and-disasters/dust-storms, last access: 16 December 2019). Strong dust storms started to influence the Indo Gangetic Plain on 21–24 April and 19 May 2015, respectively. This minimises the uncertainties resulting from dust storm simulation and permits a stronger focus on anthropogenic emissions. Resuspended dust from road traffic is also a major contributor to PM$_{2.5}$ in Delhi, and this is estimated and included in the emission inventory, as described below.

The model configuration follows the study of Marrapu et al. (2014), and the parameterisations used are listed in Table 1. Three nested domains are used, with coverage of southern Asia (45 km resolution), the Indo Gangetic Plain (15 km resolution), and the National Capital Region (5 km resolution; see Fig. 1). A test simulation with a fourth domain over Delhi at 1.67 km resolution suggests that a further increase

in resolution does not substantially improve model performance (details in Sect. S1 in the Supplement), and this is in line with results from a previous study (Mohan and Bhati, 2011). The Carbon Bond Mechanism version Z (CBMZ; Zaveri and Peters, 1999) coupled with the MOSAIC (Zaveri et al., 2008) aerosol module with four size bins is used to represent gaseous chemical reaction and aerosol chemical and dynamical processes. We neglect wet scavenging and cloud chemistry processes here, as the impact of these is likely to be negligible during the dry pre-monsoon period over India. No precipitation was recoded in Delhi during the simulation period.

The initial and boundary conditions for chemical species are provided from MOZART-4 global results (https://www.acom.ucar.edu/wrf-chem/mozart.shtml, last access: 16 December 2019). Our baseline simulation is driven by the European Centre for Medium-Range Weather Forecasts (ECMWF) meteorological data, as we find that these reproduce regional meteorology better than those from the National Centers for Environmental Prediction (NCEP) over India, consistent with a recent study (Chatani and Sharma, 2018). The ECMWF reanalysis dataset (ERA-Interim) assimilates observations with a number of nearly 10^7 per day (Dee et al., 2011) and is used for grid nudging and as initial and boundary conditions for WRF-Chem at horizontal and temporal resolutions of $0.75° \times 0.75°$ and 6 h, respectively. The wind pattern and temperature over Delhi in May 2015 are generally captured well in simulations driven by either

Table 1. Configuration of WRF-Chem.

Physics	WRF option
Microphysics	Lin scheme (Lin et al., 1983)
Surface layer	MM5 similarity
Boundary layer	Yonsei University Scheme (YSU) (Hong et al., 2006)
Cumulus	Grell 3-D
Urban	Three-category Urban Canopy Model (UCM)
Shortwave radiation	Goddard shortwave (Chou et al., 1998)
Longwave radiation	Rapid radiative transfer model
Chemistry and aerosol	**Chem option**
Gas-phase mechanism	CBMZ (Zaveri and Peters, 1999)
Aerosol module	MOSAIC with four bins ($\sim$ 40 nm to 10 µm) (Zaveri et al., 2008)
Photolysis rate	Fast-J photolysis scheme (Wild et al., 2000)
Emission inventories	
Anthropogenic emissions	SAFAR-2015 Delhi and EDGAR-HTAP v2.2
Biogenic emissions	MEGAN (Guenther et al., 2006)
Biomass burning emissions	FINN (Wiedinmyer et al., 2011)

meteorological dataset, but the model captures the variation in relative humidity much better ($R = 0.7$) with ECMWF data than with NCEP data ($R = 0.4$; negative bias of 20 %–40 %). A more detailed discussion is provided in Sect. S2.

The high-resolution Fire INventory from NCAR (FINN; Wiedinmyer et al., 2011) is adopted to provide biomass burning emissions. Interactive biogenic emissions are included using the Model of Emissions of Gases and Aerosols from Nature (MEGAN; Guenther et al., 2006). The global Emission Database for Global Atmospheric Research with Task Force on Hemispheric Transport of Air Pollution (EDGAR-HTAP; Janssens-Maenhout et al., 2015) version 2.2 (year 2010) at $0.1° \times 0.1°$ resolution is used to represent anthropogenic emissions apart from over Delhi, where they are represented by a high-resolution monthly inventory for 2015 developed under the System of Air Quality and Weather Forecasting and Research (SAFAR) project (Sahu et al., 2011, 2015). In the absence of a diurnal variation in emissions specific to Delhi, we adopt diurnal variations from Europe in this study (Denier van der Gon et al., 2011). The SAFAR inventory provides emission fluxes of PM_{10}, $PM_{2.5}$, black carbon, organic carbon, NO_x, CO, SO_2 and NMVOCs (non-methane volatile organic compounds) from five sectors, including power (POW), industry (IND), domestic and residential (DOM), traffic (TRA), and wind-blown dust (WBD) from roads. Wind-blown dust includes dust resuspended from vehicle movement on paved and unpaved roads (Sahu et al., 2011) and is therefore closely related to traffic emissions, and we combine this into the traffic sector for our study.

The NMVOC emissions are speciated according to the EDGAR (v4.3.2) global inventory (Huang et al., 2017) and

are then lumped for the CBMZ chemistry scheme. The speciation mapping is detailed in Table 2 and described below, and a toolkit has been developed to perform this mapping. Emissions of alcohols and ethers are split 20 % : 80 % between methanol and ethanol by mass and then converted into molar emissions with a fractionation based on Murrells et al. (2009). Emissions of paraffin carbon (PAR) are calculated by converting mass emissions from each VOC group into molar emissions and then multiplying by the number of paraffin carbons in order to conserve carbon. Hexanes and higher alkanes are converted into molar emissions of hexane and then multiplied by 6 to give PAR emissions. Other alkenes are mapped to molar emissions of butane, and this is then apportioned between terminal olefin carbons (OLET), internal olefin carbons (OLEI) and PAR on a molar ratio of 1 : 1 : 4, following Zaveri and Peters (1999). Ketones are split 60 % : 40 % by mass between acetone (KET) and methylethyl ketone (MEK) and then converted into molar emissions with fractions based on Murrells et al. (2009). As MEK is not included in the CBMZ mechanism, we apportion molar emissions of MEK equally between KET and PAR.

2.2 Observational network

Air quality and meteorological monitoring networks are operated in Delhi under the SAFAR project coordinated by IITM (Ministry of Earth Sciences, government of India). Measurements of $PM_{2.5}$, O_3 and NO_x during the May 2015 simulation period are available from six monitoring stations in Delhi: Dr. CV Raman University (CVR), Delhi University (DEU), Indira Ghandi International Airport Terminal 3 (AIR), Aya Nagar (AYA), NCMRWF (NCM) and

Table 2. Map of NMVOC from EDGAR emission to CBMZ scheme.

EDGAR name	Description	CBMZ (mol)
VOC1	Alcohols	20 % CH$_3$OH
		80 % C$_2$H$_5$OH
VOC2	Ethane	C$_2$H$_6$
VOC3	Propane	PAR*3
VOC4	Butane	PAR*4
VOC5	Pentane	PAR*5
VOC6	Hexanes and other alkanes	PAR*6
VOC7	Ethene	ETH
VOC8	Propene	OLET + PAR
VOC9	Ethyne	PAR*2
VOC10	Isoprene	ISOP
VOC11	Monoterpenes	ISOP*2
VOC12	Other alkenes	OLEI*0.5 + OLET*0.5 + PAR*2
VOC13	Benzene	TOL-PAR
VOC14	Toluene	TOL
VOC15	Xylenes	XYL
VOC16	Trimethylbenzenes	XYL + PAR
VOC17	Other aromatics	XYL + PAR
VOC18	Esters	RCOOH
VOC19	Ethers	20 % CH$_3$OH
		80 % C$_2$H$_5$OH
VOC21	Formaldehyde	HCHO
VOC22	Other aldehydes	ALD2
VOC23	Ketones	60 % KET
		40 % KET + PAR
VOC24	Alkanoic acids	RCOOH

Pusa (PUS). The instruments are calibrated and measurements are quality controlled in the SAFAR project (http://safar.tropmet.res.in, last access: 16 December 2019); more details are given in previous studies (Sahu et al., 2011; Beig et al., 2013; Aslam et al., 2017). Site locations are shown in Fig. 2, and measured variables are given in Table S1 in the Supplement.

2.3 Global sensitivity analysis of urban air pollution

We perform global sensitivity analysis (GSA; Iooss and Lemaître, 2015) to quantify the sensitivity of modelled outputs (PM$_{2.5}$ and O$_3$ for this study) to changes in the model inputs, which for this study are emissions from the different emission sectors. One-at-a-time sensitivity analysis is a common way of calculating model sensitivity and involves varying a single model input while the other inputs are fixed at nominal values, e.g. Wild (2007). While one-at-a-time approach is relatively easy to implement, it assumes that the model response to different inputs is independent, and this can lead to biased results (Saltelli et al., 1999; Pisoni et al., 2018; Carslaw et al., 2013). GSA overcomes the problems of the one-at-a-time approach by averaging over the other inputs rather than fixing them at specific values. This allows calculation of first-order sensitivity indices (SIs) for each variable,
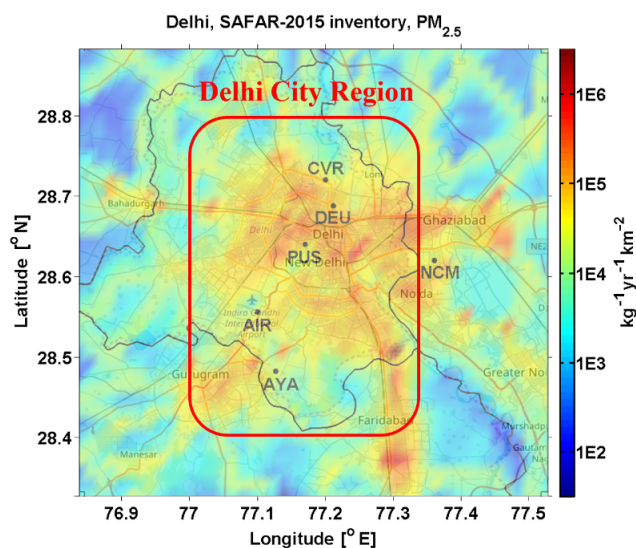

Figure 2. SAFAR inventory of total PM$_{2.5}$ emissions. The locations of measurement sites over Delhi are marked by black dots, and the Delhi city region is marked by a red box. This figure is modified from OpenSteetMap. © OpenStreetMap contributors 2019. Distributed under a Creative Commons BY-SA License.

corresponding to the ith input variable and the jth output point, given by Eq. (1) (Ryan et al., 2018):

$$SI_{i,j} = \frac{\text{Var}\left[E\left(y_j | x_i\right)\right]}{\text{Var}\left(y_j\right)} \times 100\%, \tag{1}$$

where x_i is the ith element of the input, and y_j is the jth element of the output. "$E(\cdot)$" and "$\text{Var}(\cdot)$" denote the mathematical functions that calculate the expectation and variance, respectively. The simplest way of computing $SI_{i,j}$ is by brute force, but this is also the most computationally intensive (Ryan et al., 2018).

The extended Fourier amplitude sensitivity test (eFAST), first developed by Saltelli et al. (1999), is a commonly used approach to perform GSA and calculate SIs and is adopted in this study because of its high efficiency. A basic overview and detailed equations of the eFAST method are given in the Sect. 2.2.2 of Ryan et al. (2018). A challenge of using eFAST is that it typically requires thousands of model runs. To overcome this, we employ a computationally cheaper surrogate model in place of our expensive simulation model WRF-Chem. A surrogate model is a simple model (usually statistical) which can map the inputs to the outputs of the simulation model with sufficiently good accuracy, given the same inputs. In this study, we choose a type of surrogate model called a Gaussian process emulator, which works like a function for multidimensional interpolation and has been used extensively in many areas of applied science (Carslaw et al., 2013; Koehler and Owen, 1996; Queipo et al., 2005; Vanuytrecht and Willems, 2014; Vu et al., 2015; Degroote et al., 2012) and uncertainty assessments of atmospheric models (Lee et al., 2011, 2012, 2016). Gaussian process emulators typically require a relatively small number of runs of the computationally expensive model to generate; this is in contrast to other surrogate modelling approaches, such as neural networks, which typically require thousands of model runs to train them. For a basic overview of a Gaussian process emulator, see O'Hagan (2006); a detailed introduction and equations are also given in the Sect. 2.3 of Ryan et al. (2018). Before using the emulator in place of the WRF-Chem model to carry out the thousands of model runs required for GSA, we train the emulator using a relatively small number of WRF-Chem model runs. Following previous studies (Carslaw et al., 2013; Lee et al., 2016), a maximin Latin hypercube space-filling design is employed to select the designs of training runs for WRF-Chem. Latin hypercube sampling is a statistical method for generating a near-random sample of parameter values from a multidimensional distribution (Shields and Zhang, 2016). Here, we search through 100 000 Latin hypercube random designs to find the optimal one, where the parameter space is filled most effectively. This ensures that the sets of inputs chosen cover as large a fraction of the input space as possible. Full details (including R codes) of how to generate the Gaussian process emulator, eFAST method and GSA can be found in Ryan et al. (2018).

In this study, we focus on a limited number of the emission sectors to demonstrate the effectiveness of the approach: domestic or residential emissions in Delhi (DOM), traffic emissions in Delhi (TRA, including WBD), power and industry in Delhi (POW + IND), and total emissions in the NCR outside Delhi. NCR represents the contribution of regional transport to pollution in Delhi. According to the SA-FAR emission inventory, the total PM$_{2.5}$ emissions of DOM, TRA, POW+IND and NCR are about 1.8, 6.1, 3.1 and 8.5 Gg per month in May 2015, respectively. The Gaussian process emulator is trained using 20 executions of the WRF-Chem model, with emission scaling drawn from a variation range of 0 %–200 % for each of the four specified sectors (Table S2). Emulation of the impacts of mitigation scenarios on PM$_{2.5}$ and O$_3$ can be performed in minutes on a laptop, in contrast to simulations with WRF-Chem, which require a few days on a high-performance computing cluster. The accuracy of the emulator as a surrogate of the WRF-Chem model is evaluated using a "leave-one-out" cross validation (Bastos and O'Hagan, 2009). This involves training the emulator using 19 out of the 20 sets of inputs and outputs from the WRF-Chem model runs and then evaluating the emulator against the 20th simulation. This process is carried out for each of the 20 sets of inputs and outputs. Given that the output space is multidimensional (i.e. modelled O$_3$ and PM$_{2.5}$ varied spatially and in time), the emulator is validated by comparing 10 000 (random samples varied spatially and in time) emulator output values against the corresponding output values of the WRF-Chem model. The emulator validation plot is shown in Fig. 3. Modelled and emulated O$_3$ and PM$_{2.5}$ lie very close to the 1 : 1 line with R^2 values of more than 95 %, as shown in Fig. 3, indicating that the emulation provides an accurate representation of the input–output relationship of the WRF-Chem model.

2.4 Response surfaces

Response surfaces are useful for investigating the relationship between model inputs and outputs, in this case between sectoral emissions and modelled pollutant concentrations. They have been widely applied for air quality studies and policymaking (EPA, 2006a, b, Zhao et al., 2017; Xing et al., 2017). Here, we analyse the responses of PM$_{2.5}$ and O$_3$ to changes in emissions from each sector of between 0 % and 200 %. The computationally efficient Gaussian process emulation enables us to generate response surfaces without the computational burden of a large number of runs of the WRF-chem model.

2.5 Outline of analysis

We use the WRF-Chem model to simulate the hourly concentrations of O$_3$ and PM$_{2.5}$ over the Delhi region during 2–15 May 2015 and evaluate the results against observations. We perform a simple sensitivity analysis to investigate the
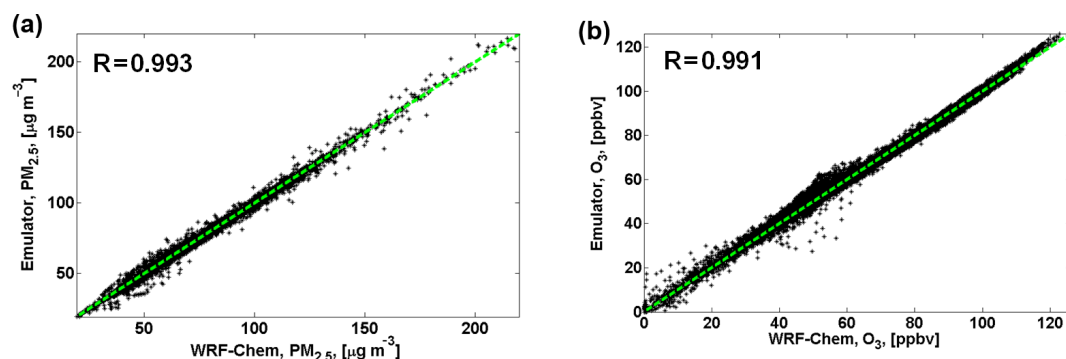
Figure 3. Validation of Gaussian process emulator with WRF-Chem model. **(a)** PM$_{2.5}$; **(b)** O$_3$. The green dashed line indicates the 1 : 1 line.
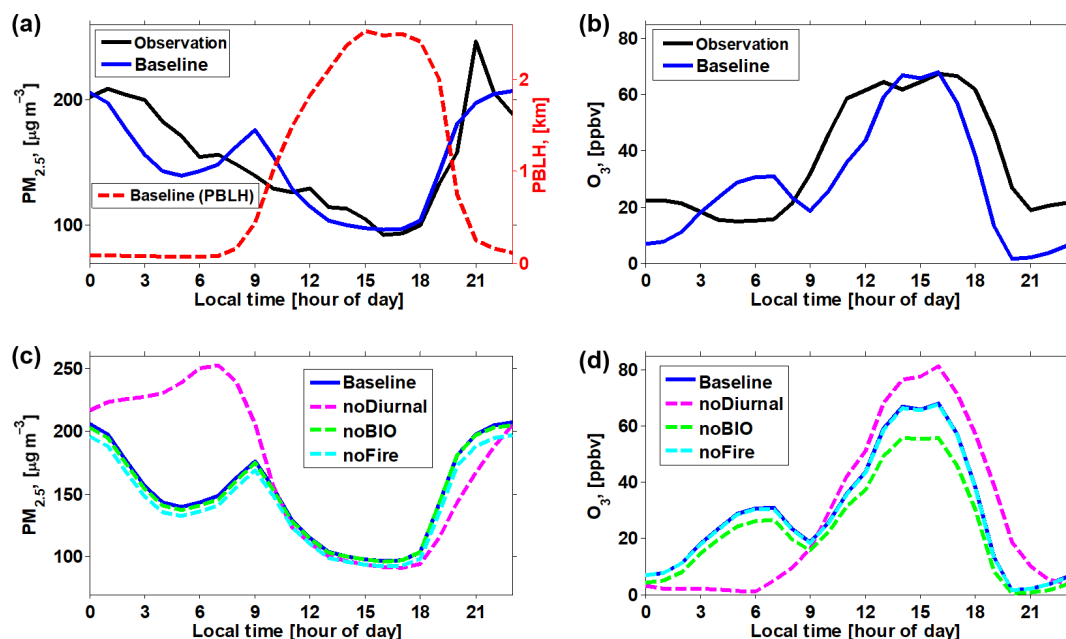

Figure 4. Average diurnal patterns of pollutants during the 2–15 May 2015 simulation period. **(a)** Modelled and observed PM$_{2.5}$ and model PBL height (PBLH), **(b)** O$_3$, **(c)** results of sensitivity studies for PM$_{2.5}$, and **(d)** results of sensitivity studies for O$_3$. **(a)** and **(c)** are for site CVR, and **(b)** and **(d)** are for site AIR (marked in Fig. 2). The sensitivity runs "noFire" and "noBIO" show model results without biomass burning and biogenic emissions, respectively, and "noDiurnal" shows model results with constant anthropogenic emissions rates throughout the day.

contributions of biomass burning and biogenic emissions to PM$_{2.5}$ and O$_3$ in Delhi. We then conduct a global sensitivity analysis, using the eFAST method (see Sect. 2.3) along with Gaussian process emulation to determine the sensitivity of modelled O$_3$ and PM$_{2.5}$ concentrations to changes in the dominant anthropogenic emission sectors. Finally, we generate response surfaces to identify appropriate mitigation strategies for reducing PM$_{2.5}$ while minimising the risks from O$_3$ increase.

3 Results and discussion

3.1 Model performance

The WRF-Chem model captures the general magnitude and variation in PM$_{2.5}$ well (Fig. 4a), with a mean bias and error of about -3.5% and 11%, respectively and an index of agreement (Willmott et al., 2012) of 75%. The frequency distributions of modelled PM$_{2.5}$ are also similar to the observations, with differences in mean and median concentrations of less than 10%, although high concentration spikes are missed by the model (Fig. S1 in the Supplement). The modelled PM$_{2.5}$ peaks at around 09:00 LT (local time) because the rush hour enhances traffic emissions before the planetary

boundary layer (PBL) height has increased (Fig. 4a). This is also seen in the modelled results at DEU (Fig. S2), which is closer to a motorway and shows a more intense PM$_{2.5}$ peak in the morning rush hour. PM$_{2.5}$ is overestimated during the morning rush hour (around 09:00 LT) and underestimated during the early morning (03:00–05:00 LT; Figs. 4a and S2). This may suggest that there is an earlier rush hour or more traffic activity at night in Delhi than in European cities, since we adopted European diurnal emission patterns in this study in the absence of local information. Detailed studies of traffic emissions and their variation in Delhi would help improve these model simulations.

The modelled chemical composition of PM$_{2.5}$ is shown in Fig. S3. Secondary inorganic aerosol (SIA), including sulfate, nitrate and ammonium, only contributes $\sim 25\%$ of aerosol mass in our simulation. In the absence of particle inorganic composition measurements during the simulation period, we compare our results with a previous modelling study of Delhi during the post-monsoon season (Marrapu et al., 2014), which also shows a $\sim 25\%$ contribution of SIA to PM$_{2.5}$ loading, in line with our results. Furthermore, our results are also consistent with an observational study, which reported the mass fraction of organic matter (usually calculated as 1.4 times organic carbon, OC) and elemental carbon (usually equivalent to black carbon in modelling studies; Chen et al., 2016b) in PM$_{2.5}$ of $\sim 20\%$ and $\sim 6\%$ in Delhi during May 2015, respectively (Sharma et al., 2018).

The model captures the peak O$_3$ well, with a bias of less than 5%, although it underestimates O$_3$ during night-time (Fig. 4b). In general, the diurnal pattern and magnitude of O$_3$ are captured by WRF-Chem (Fig. 4b), with a normalised mean bias and error of about -20% and 35%, respectively, and an index of agreement of 65%. The underestimation during night-time is likely to be because NO$_x$ is overestimated by a factor of 2–3 at night (Fig. S4), and the excess NO depletes O$_3$. This is indicated by the frequency distribution of O$_3$ and NO$_x$ (Fig. S5), where the median values of observed O$_3$ and NO$_x$ are matched well by the model. However, the higher peaks of modelled NO$_x$ concentration lower the modelled O$_3$ levels, indicating that Delhi is in the VOC-limited photochemical regime. Similar results are found at AYA (Fig. S6). The larger underestimation of O$_3$ at NCM (Fig. S5d; industrial environment site) suggests that NO$_x$ emission from the industry sector may be overestimated.

3.2 Impacts of biogenic and biomass burning emissions

Before exploring the importance of the four selected anthropogenic emission sectors on PM$_{2.5}$ and O$_3$ in Delhi during the simulation period, we investigate the contributions from other factors (biomass burning and biogenic emissions). We turn off these sources in the WRF-Chem simulation and find that there is a negligible contribution from biogenic emissions to PM$_{2.5}$ concentrations over Delhi in this season (Fig. 4c and d). It is worth noting that biogenic emis-

sions may contribute to secondary organic aerosol (SOA) in Delhi, but the formation of SOA is not represented well by the CBMZ–MOSAIC chemistry–aerosol mechanisms used in this study. However, this weakness is not expected to have a major influence on our pre-monsoon results; as described above, the difference of organic matter fraction between simulation and observation (Sharma et al., 2018) in May 2015 is less than 5%. About 10% of PM$_{2.5}$ in Delhi is derived from biomass burning during the simulation period. Crop burning in Haryana and Punjab states is a major source of this (Jethva et al., 2018; Cusworth et al., 2018). In contrast, there is a negligible contribution from biomass burning to O$_3$. However, there is a 15%–20% contribution to O$_3$ from biogenic emission of VOCs, highlighting the fact that O$_3$ production in Delhi is strongly VOC-limited.

3.3 Effect of the diurnal variation in emissions

In order to investigate the competing influences of meteorology and human activities on the diurnal patterns of PM$_{2.5}$ and O$_3$ over Delhi, we test the effect of removing the diurnal variation in anthropogenic emissions ("noDiurnal"; see Fig. 4c and d). Modelled PM$_{2.5}$ concentrations are very similar to the "baseline" run during daytime, when the PBL is well developed, with differences of less than 5%. This suggests that meteorological processes such as vertical mixing, advection and transport are the dominant factors controlling PM$_{2.5}$ in the daytime. In contrast, freshly emitted pollutants are trapped at night when the PBL is shallow, and concentrations are very sensitive to the emission flux so that the diurnal pattern of emissions is the dominant factor at night. The PM$_{2.5}$ concentration is almost doubled in the early morning (03:00–09:00 LT; Fig. 4c), when the PBL is shallow and emissions in the noDiurnal case are higher. There is also a large increase in NO$_x$ in the early morning (Fig. S4), which leads to greater depletion of O$_3$ (Fig. 4d). However, the concentration of O$_3$ is about 20%–25% higher during the ozone peak hour in the afternoon in the noDiurnal case, as the daytime NO$_x$ emissions are less (Fig. S4). This sensitivity test also highlights the VOC-limited nature of O$_3$ production in Delhi.

3.4 Sensitivity analysis of pollutants in Delhi

The importance of each anthropogenic emission sector to pollutant concentrations in Delhi is investigated using global sensitivity analysis and indicated by global sensitivity indices (SIs), as shown in Fig. 5. The sensitivity index is a measure of the contribution of the variation in pollutants from one emission sector to the total variation across all four sectors considered here. A larger SI indicates a larger influence from the corresponding sector to the modelled average surface PM$_{2.5}$ or O$_3$ over the Delhi city region (marked in Fig. 2) in this study.
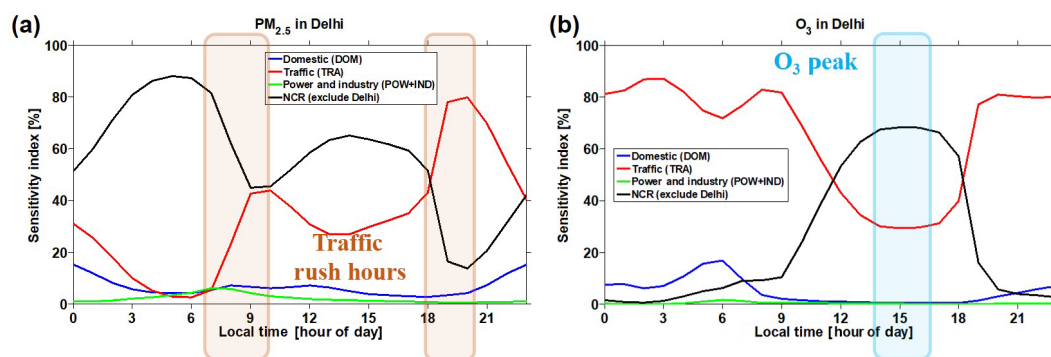
Figure 5. Averaged diurnal pattern of global sensitivity indices during the 2–15 May simulation period. **(a)** PM$_{2.5}$; **(b)** O$_3$. The PM$_{2.5}$ and O$_3$ results are averaged over Delhi city region (marked with red box in Fig. 2). The morning and evening rush hours and the period of peak ozone are marked with the boxes to highlight the notable changes in contribution from each emission sector.
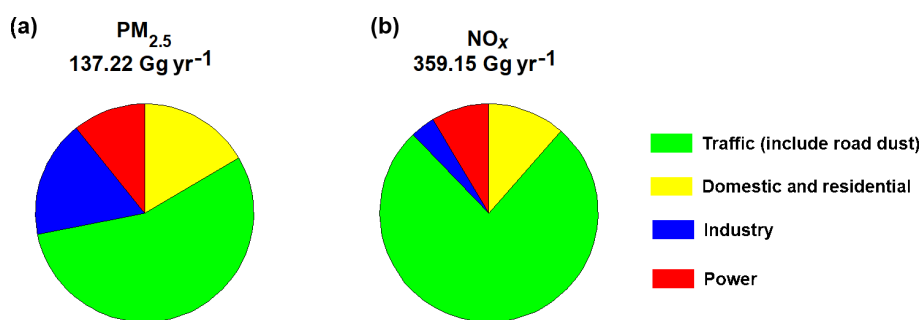

Figure 6. Annual emission of different sectors in Delhi from SAFAR inventory. **(a)** PM$_{2.5}$; **(b)** NO$_x$. The emissions of black carbon, organic carbon, non-methane VOC (NMVOC) and SO$_2$ are given in Fig. S13.

The PM$_{2.5}$ concentration is most sensitive to emissions from the NCR region surrounding Delhi, with a sensitivity index higher than 50 % most of time (Fig. 5a) and reaching 80 %–90 % and ~ 60 % during 03:00–07:00 LT and 12:00–17:00 LT, respectively. During the rush hours in the morning and evening, the sensitivity to NCR emissions is lower, while the sensitivity to Delhi traffic emissions increases by ~ 30 %. Around 10:00 LT, local traffic emissions and emissions from NCR have a similar effect on PM$_{2.5}$. In contrast, local traffic emissions dominate the PM$_{2.5}$ in Delhi around 20:00 LT, with a sensitivity contribution of up to ~ 80 %. This is caused by the collapse of the PBL in the evening rush hour at around 20:00 LT, which enhances the sensitivity to fresh local emissions. Local traffic emissions contribute ~ 60 % of primary PM$_{2.5}$ emission in Delhi (Fig. 6a), which remains concentrated in the PBL during rush hours. In contrast, the fully developed PBL in the daytime mixes air down from the free troposphere (Chen et al., 2016a), where regional transport of pollutants from NCR can be important. This could explain the second peak in the sensitivity to NCR emissions (50 %–60 %) during the afternoon (Fig. 5a).

The variation in O$_3$ in the Delhi city region is overwhelmingly dominated by local traffic emissions, with a sensitivity index higher than 80 % at night-time (Fig. 5b), when O$_3$ and traffic emissions are anti-correlated. Traffic contributes ~ 75 % of total NO$_x$ emission in Delhi (Fig. 6b), and the shallow PBL during the night traps the NO$_x$. This removes O$_3$ through chemical reaction in the absence of solar radiation. As the PBL develops in the morning, the sensitivity of O$_3$ to traffic decreases and the sensitivity to NCR emissions increases. The sensitivity to NCR emissions reaches its highest point (70 %) when the PBL is fully developed at around 15:00 LT. As discussed above, the downward mixing of air from the free troposphere and dilution of local emissions in the fully developed PBL could be the reason for this. The O$_3$ peak coincides with the highest PBL at this time because photolysis and development of the PBL are both driven by solar radiation. The development of the PBL increases the contribution from regional transport, and precursors emitted from the NCR are one of the dominant contributors to the peak of O$_3$ in Delhi. NO$_x$, mainly originating from traffic emissions, is underestimated by ~ 30 % during the O$_3$ peak period (Fig. S4). This uncertainty can propagate into the Gaussian process emulator and could lead to underestimation of the influence of traffic on peak O$_3$ but is not expected to change the nature of our conclusion about the predominance of regional transport and local traffic emissions. In addition, it is noteworthy that the NO$_x$-rich urban plume from Delhi

has a substantial influence on O_3 in downwind regions across the NCR as well, as discussed in Sect. S3.

3.5 Mitigation strategies

To demonstrate a framework for developing better mitigation strategies for addressing both $PM_{2.5}$ and O_3 pollution in Delhi, emission-sector-based pollutant response surfaces are generated using Gaussian process emulation (Fig. 7). For local emissions in Delhi, we focus mainly on traffic and residential sectors here because we find that power and industrial emissions have a more limited influence on $PM_{2.5}$ and O_3 concentrations in Delhi (Fig. 5). A range of different mitigation strategies are analysed, aiming at mitigating $PM_{2.5}$ pollution whilst minimising the risk of O_3 increase.

We find that the responses of $PM_{2.5}$ and O_3 to each emission sector are nearly linear in Delhi. The response surfaces show that reducing local traffic emissions in Delhi leads to an efficient decrease in $PM_{2.5}$ loading (Fig. 7a) but increases O_3 greatly (Fig. 7b). Reducing local domestic emissions decreases $PM_{2.5}$ loading less than reducing traffic but without increasing O_3. The small impact on O_3 may be because domestic emissions are not a major source of NO_x, contributing only 15 % of that from traffic (Fig. 6). A 10 %–20 % reduction in NO_x is expected when reducing local domestic emissions by 50 %; however a 35 %–45 % reduction is seen for a 50 % reduction in local traffic emissions (Fig. S7). In addition, VOC is reduced more than NO_x when controlling domestic emissions, as the VOC / NO_x emission ratio ($kg\,kg^{-1}$) is 1.8 in contrast to a ratio of 0.4 for traffic emissions. Greater reduction of VOC suppresses the increase in O_3 in Delhi, which is a VOC-limited environment. A reduction in local traffic emissions alone of 50 % could decrease Delhi $PM_{2.5}$ loading by 15 %–20 %, but this would also increase O_3 by 20 %–25 %. We note that our model may underestimate the influence of traffic emissions on O_3 to some extent, as described above (Sect. 3.4), suggesting that the ozone increase could be stronger than we predict. To prevent the side effect of increasing O_3 by controls on traffic emissions, regional cooperation would be required to reduce emissions in the NCR region surrounding Delhi by 25 %–30 %, which also permits a further reduction of $PM_{2.5}$ by 5 %–10 % (Fig. 7c and d). This is consistent with a recent study showing that $\sim$ 60 % of $PM_{2.5}$ in Delhi originates from outside (Amann et al., 2017). We test this by performing an additional run with WRF-Chem, using emission reductions of 50 % and 30 % for sectors of local traffic and the surrounding NCR region, respectively. We compare the WRF-Chem results of the additional run and the base case (without change of emissions) against the corresponding results from Gaussian process emulator (Fig. S8). We find that the $PM_{2.5}$ and O_3 results from the model runs lie within 5 % of those estimated with the emulator and with R^2 higher than 95 %, demonstrating the high quality of the emulation approach adopted here and underlining its deeper value for identify-

ing mitigation approaches. The suggested regional joint mitigation with NCR surrounding Delhi is in line with a recent study for mitigating $PM_{2.5}$ in Beijing, which showed that regional coordination over the North China Plain could lead to a reduction in $PM_{2.5}$ of up to 40 % in winter (Liu et al., 2016).

4 Summary

Previous studies have shown that emission controls focusing on mitigation of $PM_{2.5}$ may result in substantial increases in surface ozone over urban areas that are in a VOC-limited photochemical environment. Comprehensive studies of mitigation strategies with respect to both $PM_{2.5}$ and O_3 are urgently required but are limited in India. In this study, we demonstrate a numerical framework for informing emission-sector-based mitigation strategies in Delhi that account for multiple pollutants.

By using Gaussian process emulation with an air quality model (WRF-Chem), we generate a computationally efficient surrogate model for performing global sensitivity analysis and calculating emission-sector-based pollutant response surfaces. These enable us to exhaustively investigate the impacts of different mitigation scenarios on $PM_{2.5}$ and O_3 in Delhi, which help decision makers choose better mitigation strategies. Global sensitivity analysis shows that pollutants originating from the National Capital Region (NCR) surrounding Delhi and local traffic emissions are the major contributors of $PM_{2.5}$ and O_3 in Delhi. They co-dominate the O_3 peak and $PM_{2.5}$ in Delhi during daytime, while the regional transport governs $PM_{2.5}$ during the night, in line with a recent study showing that $\sim$ 60 % of $PM_{2.5}$ in Delhi originates from outside (Amann et al., 2017). Controlling local traffic emissions in Delhi would have the notable side effect of increasing O_3, at least in the pre-monsoon and summer period (peak O_3 season) that we consider here. This is in line with recent increases in O_3 seen in China (Silver et al., 2018; Li et al., 2018). The Chinese experience suggests that regional joint coordination is required to effectively mitigate $PM_{2.5}$ pollution in Beijing (Liu et al., 2016). Our pollutant response surfaces go one step further and suggest that joint coordinated emission controls with the NCR region surrounding Delhi would be required to not only achieve a more ambitious reduction of $PM_{2.5}$ but also to minimise the risk of O_3 increases. In the regional joint coordination, residential energy use could be a dominant emission sector over a large region in India (Conibear et al., 2018).

5 Discussion

The experiences of developed countries (Dooley, 2002; EPA, 2011) and recently in China (J. Huang et al., 2018; Wang et al., 2019) show that regional joint coordination can be achieved by changing energy infrastructure (e.g. replacing
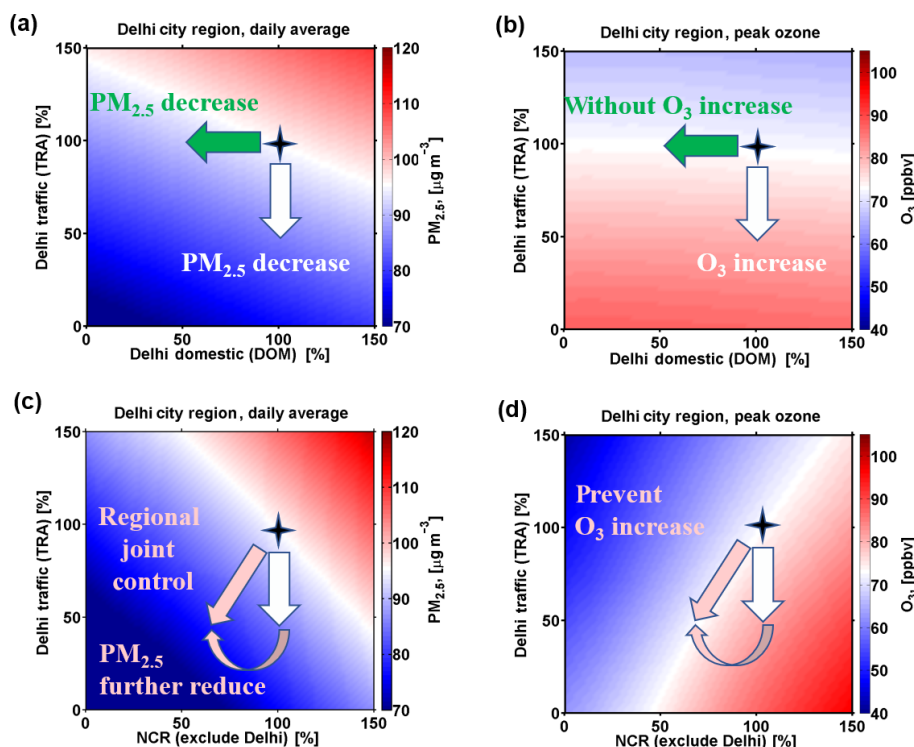
Figure 7. Response surfaces for PM$_{2.5}$ and ozone concentrations over Delhi city region, averaged over 2–15 May 2018. **(a)** Daily average of PM$_{2.5}$ concentrations as a function of local traffic and domestic emissions in Delhi, **(b)** peak hourly ozone concentrations as a function of local traffic and domestic emissions in Delhi, **(c)** daily average of PM$_{2.5}$ concentrations as a function of local traffic emissions in Delhi and emissions in NCR region surrounding Delhi, and **(d)** peak hourly ozone concentrations as a function of local traffic emissions in Delhi and emissions in NCR region surrounding Delhi. The star indicates current conditions, and the arrows show the effect of possible emission controls.

fossil fuel by renewable energy and natural gas), desulfurisation and denitrification technologies, popularisation of new energy vehicles, strict control of vehicle exhaust, and reducing road and construction dust. Further studies with more detailed information on specific emission sectors and strategies for clean-technology development and popularisation would permit deeper insight into air pollution mitigation approaches suitable for Delhi. These are needed to address both PM$_{2.5}$, which has a higher impact on public health (e.g. J. Huang et al., 2018), and O$_3$, which greatly impacts regional ecology and agriculture (e.g. Avnery et al., 2011). A more comprehensive evaluation of the health and economic benefits of different mitigation strategies would greatly help Indian decision makers, and the framework we have demonstrated here would provide a strong foundation for this.

Author contributions. OW and YC conceived the study. YC performed the simulations and emulation and processed and interpreted the results, with help from YW. ER designed and built the Gaussian process emulator. GB and SKS provided the observations and SAFAR emission inventory. DL, AA, SAN and GM helped with preprocessing the emission data and developing the emission toolkit. VS and RSS provided useful discussion on the emission inventory. RSS led the development of the PROMOTE project. YC and OW wrote the paper, with input from all co-authors.

References

Amann, M., Bertok, I., Borken-Kleefeld, J., Cofala, J., Heyes, C., Höglund-Isaksson, L., Klimont, Z., Nguyen, B., Posch, M., Rafaj, P., Sandler, R., Schöpp, W., Wagner, F., and Winiwarter, W.: Cost-effective control of air quality and greenhouse gases in Europe: Modeling and policy applications, Environ. Model. Softw., 26, 1489–1501, https://doi.org/10.1016/j.envsoft.2011.07.012, 2011.

Amann, M., Purohit, P., Bhanarkar, A. D., Bertok, I., Borken-Kleefeld, J., Cofala, J., Heyes, C., Kiesewetter, G., Klimont, Z., Liu, J., Majumdar, D., Nguyen, B., Rafaj, P., Rao, P. S., Sander, R., Schöpp, W., Srivastava, A., and Vardhan, B. H.: Managing future air quality in megacities: A case study for Delhi, Atmos. Environ., 161, 99–111, https://doi.org/10.1016/j.atmosenv.2017.04.041, 2017.

Ashworth, K., Wild, O., and Hewitt, C. N.: Impacts of biofuel cultivation on mortality and crop yields, Nat. Clim. Change, 3, 492–496, https://doi.org/10.1038/nclimate1788, 2013.

Aslam, M. Y., Krishna, K. R., Beig, G., Tinmaker, M. I. R., and Chate, D. M.: Seasonal Variation of Urban Heat Island and Its Impact on Air-Quality Using SAFAR Observations at Delhi, India, Am. J. Clim. Change, 6, 294–305, https://doi.org/10.4236/ajcc.2017.62015, 2017.

Avnery, S., Mauzerall, D. L., Liu, J., and Horowitz, L. W.: Global crop yield reductions due to surface ozone exposure: 2. Year 2030 potential crop production losses and economic damage under two scenarios of O$_3$ pollution, Atmos. Environ., 45, 2297–2309, https://doi.org/10.1016/j.atmosenv.2011.01.002, 2011.

Bastos, L. S. and O'Hagan, A.: Diagnostics for Gaussian Process Emulators, Technometrics, 51, 425–438, https://doi.org/10.1198/TECH.2009.08019, 2009.

Beig, G., Chate, D. M., Ghude, S. D., Ali, K., Satpute, T., Sahu, S. K., Parkhi, N., and Trimbake, H. K.: Evaluating population exposure to environmental pollutants during Deepavali fireworks displays using air quality measurements of the SAFAR network, Chemosphere, 92, 116–124, https://doi.org/10.1016/j.chemosphere.2013.02.043, 2013.

Carslaw, K. S., Lee, L. A., Reddington, C. L., Pringle, K. J., Rap, A., Forster, P. M., Mann, G. W., Spracklen, D. V., Woodhouse, M. T., Regayre, L. A., and Pierce, J. R.: Large contribution of natural aerosols to uncertainty in indirect forcing, Nature, 503, 67–71, https://doi.org/10.1038/nature12674, 2013.

Chatani, S. and Sharma, S.: Uncertainties Caused by Major Meteorological Analysis Data Sets in Simulating Air Quality Over India, J. Geophys. Res.-Atmos., 123, 6230–6247, https://doi.org/10.1029/2017JD027502, 2018.

Chen, L., Guo, B., Huang, J., He, J., Wang, H., Zhang, S., and Chen, S. X.: Assessing air-quality in Beijing-Tianjin-Hebei region: The method and mixed tales of PM$_{2.5}$ and O$_3$, Atmos. Environ., 193, 290–301, https://doi.org/10.1016/j.atmosenv.2018.08.047, 2018.

Chen, Y., Cheng, Y., Ma, N., Wolke, R., Nordmann, S., Schüttauf, S., Ran, L., Wehner, B., Birmili, W., van der Gon, H. A. C. D., Mu, Q., Barthel, S., Spindler, G., Stieger, B., Müller, K., Zheng, G. J., Pöschl, U., Su, H., and Wiedensohler, A.: Sea salt emission, transport and influence on size-segregated nitrate simulation: a case study in northwestern Europe by WRF-Chem, Atmos. Chem. Phys., 16, 12081–12097, https://doi.org/10.5194/acp-16-12081-2016, 2016a.

Chen, Y., Cheng, Y. F., Nordmann, S., Birmili, W., Denier van der Gon, H. A. C., Ma, N., Wolke, R., Wehner, B., Sun, J., Spindler, G., Mu, Q., Pöschl, U., Su, H., and Wiedensohler, A.: Evaluation of the size segregation of elemental carbon (EC) emission in Europe: influence on the simulation of EC long-range transportation, Atmos. Chem. Phys., 16, 1823–1835, https://doi.org/10.5194/acp-16-1823-2016, 2016b.

Chen, Y., Wild, O., Conibear, L., Ran, L., He, J., Wang, L., and Wang, Y.: Local characteristics of and exposure to fine particulate matter (PM$_{2.5}$) in four indian megacities, Atmos. Environ., 5, 100052, https://doi.org/10.1016/j.aeaoa.2019.100052, 2020.

Chou, M., Suarez, M., Ho, C., Yan, M., and Lee, K.: Parameterizations for Cloud Overlapping and Shortwave Single-Scattering Properties for Use in General Circulation and Cloud Ensemble, Models, J. Climate, 11, 202–214, 1998.

Chowdhury, S. and Dey, S.: Cause-specific premature death from ambient PM$_{2.5}$ exposure in India: Estimate adjusted for baseline mortality, Environ. Int., 91, 283–290, https://doi.org/10.1016/j.envint.2016.03.004, 2016.

Chowdhury, S., Dey, S., Tripathi, S. N., Beig, G., Mishra, A. K., and Sharma, S.: "Traffic intervention" policy fails to mitigate air pollution in megacity Delhi, Environ. Sci. Policy, 74, 8–13, https://doi.org/10.1016/j.envsci.2017.04.018, 2017.

Conibear, L., Butt, E. W., Knote, C., Arnold, S. R., and Spracklen, D. V.: Residential energy use emissions dominate health impacts from exposure to ambient particulate matter in India, Nat. Commun., 9, 617, https://doi.org/10.1038/s41467-018-02986-7, 2018.

Cusworth, D. H., Mickley, L. J., Sulprizio, M. P., Liu, T., Marlier, M. E., DeFries, R. S., Guttikunda, S. K., and Gupta, P.: Quantifying the influence of agricultural fires in northwest India on urban air pollution in Delhi, India, Environ. Res. Lett., 13, 044018, https://doi.org/10.1088/1748-9326/aab303, 2018.

Dee, D. P., Uppala, S. M., Simmons, A. J., Berrisford, P., Poli, P., Kobayashi, S., Andrae, U., Balmaseda, M. A., Balsamo, G.,

Bauer, P., Bechtold, P., Beljaars, A. C. M., van de Berg, L., Bidlot, J., Bormann, N., Delsol, C., Dragani, R., Fuentes, M., Geer, A. J., Haimberger, L., Healy, S. B., Hersbach, H., Hólm, E. V., Isaksen, L., Kållberg, P., Köhler, M., Matricardi, M., McNally, A. P., Monge-Sanz, B. M., Morcrette, J.-J., Park, B.-K., Peubey, C., de Rosnay, P., Tavolato, C., Thépaut, J.-N., and Vitart, F.: The ERA-Interim reanalysis: configuration and performance of the data assimilation system, Q. J. Roy. Meteorol. Soc., 137, 553–597, https://doi.org/10.1002/qj.828, 2011.

Degroote, J., Couckuyt, I., Vierendeels, J., Segers, P., and Dhaene, T.: Inverse modelling of an aneurysm's stiffness using surrogate-based optimization and fluid-structure interaction simulations, Struct. Multidisc. Optimiz., 46, 457–469, https://doi.org/10.1007/s00158-011-0751-7, 2012.

Denier van der Gon, H. A. C., Hendriks, C., Kuenen, J., Segers, A., and Visschedijk, A.: TNO Report: Description of current temporal emission patterns and sensitivity of predicted AQ for temporal emission patterns, available at: https://atmosphere.copernicus.eu/sites/default/files/2019-07/MACC_TNO_del_1_3_v2.pdf (last access: 16 December 2019), 2011.

Dooley, E.: Clearing the Air over the London Fog, Environ. Health Perspect., 110, A748–A749, 2002.

Duncan, B. N., Lamsal, L. N., Thompson, A. M., Yoshida, Y., Lu, Z., Streets, D. G., Hurwitz, M. M., and Pickering, K. E.: A space-based, high-resolution view of notable changes in urban NO$_x$ pollution around the world (2005–2014), J. Geophys. Res.-Atmos., 121, 976–996, https://doi.org/10.1002/2015JD024121, 2016.

ECMWF: ECMWF interim re-analysis dataset, http://apps.ecmwf.int/datasets/data/interim-full-daily, last access: 16 December 2019.

EPA: Technical support document for the proposed mobile source air toxics rule: ozone modeling, Office of Air Quality Planning and Standards, US Environmental Protection Agency, Research Triangle Park, NC, USA, 1–12, 2006a.

EPA: Technical support document for the proposed PM NAAQS rule: Response Surface Modeling, Office of Air Quality Planning and Standards, US Environmental Protection Agency, Research Triangle Park, NC, USA, 1–25, 2006b.

EPA: Benefits and costs of the Clean Air Act 1990–2020, the second prospective study, available at: https://www.epa.gov/clean-air-act-overview/benefitsand-costs-clean-air-act-1990-2020-second-prospective-study (last access: 20 August 2018). 2011.

Fleming, Z. L., Doherty, R. M., Von Schneidemesser, E., Malley, C. S., Cooper, O. R., Pinto, J. P., Colette, A., Xu, X., Simpson, D., Schultz, M. G., Lefohn, A. S., Hamad, S., Moolla, R., Solberg, S., and Feng, Z.: Tropospheric Ozone Assessment Report: Present-day ozone distribution and trends relevant to human health, Elem. Sci. Anth., 6, p. 12, https://doi.org/10.1525/elementa.273, 2018.

Gao, M., Guttikunda, S. K., Carmichael, G. R., Wang, Y., Liu, Z., Stanier, C. O., Saide, P. E., and Yu, M.: Health impacts and economic losses assessment of the 2013 severe haze event in Beijing area, Sci. Total Environ., 511, 553–561, https://doi.org/10.1016/j.scitotenv.2015.01.005, 2015.

Gao, M., Beig, G., Song, S., Zhang, H., Hu, J., Ying, Q., Liang, F., Liu, Y., Wang, H., Lu, X., Zhu, T., Carmichael, G. R.,

Nielsen, C. P., and McElroy, M. B.: The impact of power generation emissions on ambient PM$_{2.5}$ pollution and human health in China and India, Environ. Int., 121, 250–259, https://doi.org/10.1016/j.envint.2018.09.015, 2018.

Gao, M., Sherman, P., Song, S., Yu, Y., Wu, Z., and McElroy, M. B.: Seasonal prediction of Indian wintertime aerosol pollution using the ocean memory effect, Sci. Adv., 5, 4157, https://doi.org/10.1126/sciadv.aav4157, 2019.

Ghude, S. D., Jain, S. L., Arya, B. C., Beig, G., Ahammed, Y. N., Kumar, A., and Tyagi, B.: Ozone in ambient air at a tropical megacity, Delhi: characteristics, trends and cumulative ozone exposure indices, J. Atmos. Chem., 60, 237–252, https://doi.org/10.1007/s10874-009-9119-4, 2008.

Ghude, S. D., Jena, C., Chate, D. M., Beig, G., Pfister, G. G., Kumar, R., and Ramanathan, V.: Reductions in India's crop yield due to ozone, Geophys. Res. Lett., 41, 5685–5691, https://doi.org/10.1002/2014GL060930, 2014.

Ghude, S. D., Chate, D. M., Jena, C., Beig, G., Kumar, R., Barth, M. C., Pfister, G. G., Fadnavis, S., and Pithani, P.: Premature mortality in India due to PM$_{2.5}$ and ozone exposure, Geophys. Res. Lett., 43, 4650–4658, https://doi.org/10.1002/2016GL068949, 2016.

Grell, G. A., Peckham, S. E., Schmitz, R., McKeen, S. A., Frost, G., Skamarock, W. C., and Eder, B.: Fully coupled "online" chemistry within the WRF model, Atmos. Environ., 39, 6957–6975, https://doi.org/10.1016/j.atmosenv.2005.04.027, 2005.

Guenther, A., Karl, T., Harley, P., Wiedinmyer, C., Palmer, P. I., and Geron, C.: Estimates of global terrestrial isoprene emissions using MEGAN (Model of Emissions of Gases and Aerosols from Nature), Atmos. Chem. Phys., 6, 3181–3210, https://doi.org/10.5194/acp-6-3181-2006, 2006.

Gupta, M. and Mohan, M.: Validation of WRF/Chem model and sensitivity of chemical mechanisms to ozone simulation over megacity Delhi, Atmos. Environ., 122, 220–229, https://doi.org/10.1016/j.atmosenv.2015.09.039, 2015.

Hollaway, M., Wild, O., Yang, T., Sun, Y., Xu, W., Xie, C., Whalley, L., Slater, E., Heard, D., and Liu, D.: Photochemical impacts of haze pollution in an urban environment, Atmos. Chem. Phys., 19, 9699–9714, https://doi.org/10.5194/acp-19-9699-2019, 2019.

Hong, S.-Y., Noh, Y., and Dudhia, J.: A new vertical diffusion package with an explicit treatment of entrainment processes, Mon. Weather Rev., 134, 2318–2341, 2006.

Huang, G., Brook, R., Crippa, M., Janssens-Maenhout, G., Schieberle, C., Dore, C., Guizzardi, D., Muntean, M., Schaaf, E., and Friedrich, R.: Speciation of anthropogenic emissions of non-methane volatile organic compounds: a global gridded data set for 1970–2012, Atmos. Chem. Phys., 17, 7683–7701, https://doi.org/10.5194/acp-17-7683-2017, 2017.

Huang, J., Pan, X., Guo, X., and Li, G.: Health impact of China's Air Pollution Prevention and Control Action Plan: an analysis of national air quality monitoring and mortality data, Lancet Planet. Health, 2, e313–e323, https://doi.org/10.1016/S2542-5196(18)30141-4, 2018.

Huang, X., Wang, Z., and Ding, A.: Impact of Aerosol-PBL Interaction on Haze Pollution: Multiyear Observational Evidences in North China, Geophys. Res. Lett., 45, 8596–8603, https://doi.org/10.1029/2018GL079239, 2018.

Iooss, B. and Lemaître, P.: A review on global sensitivity analysis methods, in: Uncertainty Management in Simulation optimiza-

tion of Complex Systems: Algorithms and Applications, edited by: Meloni, C. and Dellino, G., Springer, Boston, 2015.

Janssens-Maenhout, G., Crippa, M., Guizzardi, D., Dentener, F., Muntean, M., Pouliot, G., Keating, T., Zhang, Q., Kurokawa, J., Wankmüller, R., Denier van der Gon, H., Kuenen, J. J. P., Klimont, Z., Frost, G., Darras, S., Koffi, B., and Li, M.: HTAP_v2.2: a mosaic of regional and global emission grid maps for 2008 and 2010 to study hemispheric transport of air pollution, Atmos. Chem. Phys., 15, 11411–11432, https://doi.org/10.5194/acp-15-11411-2015, 2015.

Jethva, H., Chand, D., Torres, O., Gupta, P., Lyapustin, A., and Patadia, F.: Agricultural Burning and Air Quality over Northern India: A Synergistic Analysis using NASA's A-train Satellite Data and Ground Measurements, Aerosol Air Qual. Res., 18, 1756–1773, https://doi.org/10.4209/aaqr.2017.12.0583, 2018.

Khare, M., Gargava, P., and Khan, A. A.: Effect of PM$_{2.5}$ chemical constituents on atmospheric visibility impairment AU – Khanna, Isha, J. Air Waste Manage. Assoc., 68, 430–437, https://doi.org/10.1080/10962247.2018.1425772, 2018.

Koehler, J. R. and Owen, A. B.: 9 Computer experiments, in: Handbook of Statistics, Elsevier, available at: https://www.math.umd.edu/~slud/RITF17/Computer_Experiments.pdf (last access: 16 December 2019), 261–308, 1996.

Kumar, R., Barth, M. C., Madronich, S., Naja, M., Carmichael, G. R., Pfister, G. G., Knote, C., Brasseur, G. P., Ojha, N., and Sarangi, T.: Effects of dust aerosols on tropospheric chemistry during a typical pre-monsoon season dust storm in northern India, Atmos. Chem. Phys., 14, 6813–6834, https://doi.org/10.5194/acp-14-6813-2014, 2014a.

Kumar, R., Barth, M. C., Pfister, G. G., Naja, M., and Brasseur, G. P.: WRF-Chem simulations of a typical pre-monsoon dust storm in northern India: influences on aerosol optical properties and radiation budget, Atmos. Chem. Phys., 14, 2431–2446, https://doi.org/10.5194/acp-14-2431-2014, 2014b.

Kumar, R., Barth, M. C., Pfister, G. G., Delle Monache, L., Lamarque, J. F., Archer-Nicholls, S., Tilmes, S., Ghude, S. D., Wiedinmyer, C., Naja, M., and Walters, S.: How Will Air Quality Change in South Asia by 2050?, J. Geophys. Res.-Atmos., 123, 1840–1864, https://doi.org/10.1002/2017JD027357, 2018.

Lee, L. A., Carslaw, K. S., Pringle, K. J., Mann, G. W., and Spracklen, D. V.: Emulation of a complex global aerosol model to quantify sensitivity to uncertain parameters, Atmos. Chem. Phys., 11, 12253–12273, https://doi.org/10.5194/acp-11-12253-2011, 2011.

Lee, L. A., Carslaw, K. S., Pringle, K. J., and Mann, G. W.: Mapping the uncertainty in global CCN using emulation, Atmos. Chem. Phys., 12, 9739–9751, https://doi.org/10.5194/acp-12-9739-2012, 2012.

Lee, L. A., Reddington, C. L., and Carslaw, K. S.: On the relationship between aerosol model uncertainty and radiative forcing uncertainty, P. Natl. Acad. Sci. USA, 113, 5820–5827, https://doi.org/10.1073/pnas.1507050113, 2016.

Lelieveld, J., Bourtsoukidis, E., Brühl, C., Fischer, H., Fuchs, H., Harder, H., Hofzumahaus, A., Holland, F., Marno, D., Neumaier, M., Pozzer, A., Schlager, H., Williams, J., Zahn, A., and Ziereis, H.: The South Asian monsoon – Pollution pump and purifier, Science, 361, 270–273, https://doi.org/10.1126/science.aar2501, 2018.

Li, K., Jacob, D. J., Liao, H., Shen, L., Zhang, Q., and Bates, K. H.: Anthropogenic drivers of 2013–2017 trends in summer surface ozone in China, P. Natl. Acad. Sci. USA, 116, 422–427, https://doi.org/10.1073/pnas.1812168116, 2018.

Lin, Y., Farley, R., and Orville, H.: Bulk Parameterization of the Snow Field in a Cloud Model, J. Clim. Appl. Meteorol., 22, 1065–1092, 1983.

Liu, H., Wang, X. M., Pang, J. M., and He, K. B.: Feasibility and difficulties of China's new air quality standard compliance: PRD case of PM$_{2.5}$ and ozone from 2010 to 2025, Atmos. Chem. Phys., 13, 12013–12027, https://doi.org/10.5194/acp-13-12013-2013, 2013.

Liu, J., Mauzerall, D. L., Chen, Q., Zhang, Q., Song, Y., Peng, W., Klimont, Z., Qiu, X., Zhang, S., Hu, M., Lin, W., Smith, K. R., and Zhu, T.: Air pollutant emissions from Chinese households: A major and underappreciated ambient pollution source, P. Natl. Acad. Sci. USA, 113, 7756–7761, https://doi.org/10.1073/pnas.1604537113, 2016.

Liu, J., Xiang, S., Yi, K., and Tao, W.: Co-Mitigation of Ozone and PM$_{2.5}$ Pollution over the Beijing-Tianjin-Hebei Region, in: 2017 AGU Fall Meeting, New Orleans, 2017AGUFM.A53F2327L, 2017.

Lowe, D.: WRF-Chem emission tool, the University of Manchester, available at: https://github.com/douglowe/WRF_UoM_EMIT/releases/tag/v1.0, last access: 16 December 2019a.

Lowe, D.: WRF-Chem emission tool for the PROMOTE project of Delhi air quality, available at: https://github.com/douglowe/PROMOTE-emissions/releases/tag/v1.0, last access: 16 December 2019b.

Lu, X., Hong, J., Zhang, L., Cooper, O. R., Schultz, M. G., Xu, X., Wang, T., Gao, M., Zhao, Y., and Zhang, Y.: Severe Surface Ozone Pollution in China: A Global Perspective, Environ. Sci. Technol. Lett., 5, 487–494, https://doi.org/10.1021/acs.estlett.8b00366, 2018.

Marrapu, P., Cheng, Y., Beig, G., Sahu, S., Srinivas, R., and Carmichael, G. R.: Air quality in Delhi during the Commonwealth Games, Atmos. Chem. Phys., 14, 10619–10630, https://doi.org/10.5194/acp-14-10619-2014, 2014.

Menon, S., Hansen, J., Nazarenko, L., and Luo, Y.: Climate Effects of Black Carbon Aerosols in China and India, Science, 297, 2250–2253, https://doi.org/10.1126/science.1075159, 2002.

Mohan, M. and Bhati, S.: Analysis of WRF Model Performance over Subtropical Region of Delhi, India, Adv. Meteorol., 2011, 621235, https://doi.org/10.1155/2011/621235, 2011.

Mohan, M., and Gupta, M.: Sensitivity of PBL parameterizations on PM$_{10}$ and ozone simulation using chemical transport model WRF-Chem over a sub-tropical urban airshed in India, Atmos. Environ., 185, 53–63, https://doi.org/10.1016/j.atmosenv.2018.04.054, 2018.

Mukherjee, A. and Toohey, D. W.: A study of aerosol properties based on observations of particulate matter from the U.S. Embassy in Beijing, China, Earth's Future, 4, 381–395, https://doi.org/10.1002/2016EF000367, 2016.

Murrells, T. P., Passant, N. R., Thistlethwaite, G., Wagner, A., Li, Y., Bush, T., Norris, J., Walker, C., Stewart, R. A., Tsagatakis, I., Whiting, R., Conolly, C., Okamura, S., Peirce, M., Sneddon, S., Webb, J., Thomas, J., MacCarthy, J., Choudrie, S., Webb, N., and Mould, R.: UK Emissions of Air Pollutants 1970 to 2009, available at: https://uk-air.defra.gov.uk/assets/documents/

reports/cat07/1401131501_NAEI_Annual_Report_2009.pdf (last access: 12 November 2018), 2009.

NCAR: MOZART-4 global model results, available at: https://www.acom.ucar.edu/wrf-chem/mozart.shtml, last access: 16 December 2019.

NCEP/National Weather Service/NOAA/U.S. Department of Commerce: NCEP reanalysis dataset,, available at: https://rda.ucar.edu/data/ds083.2/, 2000 (updated daily).

NCEP SST: NCEP sea surface temperature, available at: https://polar.ncep.noaa.gov/sst/, last access: 16 December 2019.

O'Hagan, A.: Bayesian analysis of computer code outputs: A tutorial, Reliabil. Syst. Saf., 91, 1290–1300, https://doi.org/10.1016/j.ress.2005.11.025, 2006.

O'Hagan, A. and West, M.: Handbook of applied Bayesian analysis, Oxford University Press, New York, 2009.

Ojha, N., Naja, M., Singh, K. P., Sarangi, T., Kumar, R., Lal, S., Lawrence, M. G., Butler, T. M., and Chandola, H. C.: Variabilities in ozone at a semi-urban site in the Indo-Gangetic Plain region: Association with the meteorology and regional processes, J. Geophys. Res.- Atmos., 117, D20301, https://doi.org/10.1029/2012JD017716, 2012.

Pisoni, E., Clappier, A., Degraeuwe, B., and Thunis, P.: Adding spatial flexibility to source-receptor relationships for air quality modeling, Environ. Model. Softw., 90, 68–77, https://doi.org/10.1016/j.envsoft.2017.01.001, 2017.

Pisoni, E., Albrecht, D., Mara, T. A., Rosati, R., Tarantola, S., and Thunis, P.: Application of uncertainty and sensitivity analysis to the air quality SHERPA modelling tool, Atmos. Environ., 183, 84–93, https://doi.org/10.1016/j.atmosenv.2018.04.006, 2018.

Pope, C. A., Ezzati, M., and Dockery, D. W.: Fine-Particulate Air Pollution and Life Expectancy in the United States, New Engl. J. Med., 360, 376–386, https://doi.org/10.1056/NEJMsa0805646, 2009.

Queipo, N. V., Haftka, R. T., Shyy, W., Goel, T., Vaidyanathan, R., and Kevin Tucker, P.: Surrogate-based analysis and optimization, Progr. Aerosp. Sci., 41, 1–28, https://doi.org/10.1016/j.paerosci.2005.02.001, 2005.

Ran, L., Zhao, C., Geng, F., Tie, X., Tang, X., Peng, L., Zhou, G., Yu, Q., Xu, J., and Guenther, A.: Ozone photochemical production in urban Shanghai, China: Analysis based on ground level observations, J. Geophys. Res.-Atmos., 114, D15301, https://doi.org/10.1029/2008JD010752, 2009.

Ryan, E., Wild, O., Voulgarakis, A., and Lee, L.: Fast sensitivity analysis methods for computationally expensive models with multi-dimensional output, Geosci. Model Dev., 11, 3131–3146, https://doi.org/10.5194/gmd-11-3131-2018, 2018.

Sahu, S. K., Beig, G., and Parkhi, N. S.: Emissions inventory of anthropogenic PM$_{2.5}$ and PM$_{10}$ in Delhi during Commonwealth Games 2010, Atmos. Environ., 45, 6180–6190, https://doi.org/10.1016/j.atmosenv.2011.08.014, 2011.

Sahu, S. K., Beig, G., and Parkhi, N.: High Resolution Emission Inventory of NO$_x$ and CO for Mega City Delhi, India, Aerosol Air Qual. Res., 15, 1137–1144, https://doi.org/10.4209/aaqr.2014.07.0132, 2015.

Saltelli, A., Tarantola, S., and Chan, K. P. S.: A Quantitative Model-Independent Method for Global Sensitivity Analysis of Model Output, Technometrics, 41, 39–56, https://doi.org/10.1080/00401706.1999.10485594, 1999.

Sharma, A., Ojha, N., Pozzer, A., Mar, K. A., Beig, G., Lelieveld, J., and Gunthe, S. S.: WRF-Chem simulated surface ozone over south Asia during the pre-monsoon: effects of emission inventories and chemical mechanisms, Atmos. Chem. Phys., 17, 14393–14413, https://doi.org/10.5194/acp-17-14393-2017, 2017.

Sharma, S. K., Mandal, T. K., Sharma, A., Jain, S., and Saraswati: Carbonaceous Species of PM$_{2.5}$ in Megacity Delhi, India During 2012–2016, Bull. Environ. Contam. Toxicol., 100, 695–701, https://doi.org/10.1007/s00128-018-2313-9, 2018.

Shields, M. D. and Zhang, J.: The generalization of Latin hypercube sampling, Reliabil. Eng. Syst. Saf., 148, 96–108, https://doi.org/10.1016/j.ress.2015.12.002, 2016.

Silver, B., Reddington, C. L., Arnold, S. R., and Spracklen, D. V.: Substantial changes in air pollution across China during 2015–2017, Environ. Res. Lett., 13, 114012, https://doi.org/10.1088/1748-9326/aae718, 2018.

Stafoggia, M., Bellander, T., Bucci, S., Davoli, M., de Hoogh, K., de' Donato, F., Gariazzo, C., Lyapustin, A., Michelozzi, P., Renzi, M., Scortichini, M., Shtein, A., Viegi, G., Kloog, I., and Schwartz, J.: Estimation of daily PM$_{10}$ and PM$_{2.5}$ concentrations in Italy, 2013–2015, using a spatiotemporal land-use random-forest model, Environ. Int., 124, 170–179, https://doi.org/10.1016/j.envint.2019.01.016, 2019.

Thunis, P., Degraeuwe, B., Pisoni, E., Ferrari, F., and Clappier, A.: On the design and assessment of regional air quality plans: The SHERPA approach, J. Environ. Manage., 183, 952–958, https://doi.org/10.1016/j.jenvman.2016.09.049, 2016.

Turner, M. C., Jerrett, M., Pope, C. A., 3rd, Krewski, D., Gapstur, S. M., Diver, W. R., Beckerman, B. S., Marshall, J. D., Su, J., Crouse, D. L., and Burnett, R. T.: Long-Term Ozone Exposure and Mortality in a Large Prospective Study, Am. Journal Respirat. Crit. Care Med., 193, 1134–1142, https://doi.org/10.1164/rccm.201508-1633OC, 2016.

Vanuytrecht, E. and Willems, P.: Global sensitivity analysis of yield output from the water productivity model, Environ. Model. Softw., 51, 323–332, https://doi.org/10.1016/j.envsoft.2013.10.017, 2014.

Vu, N., Rafiee, R., Zhuang, X., Lahmer, T., and Rabczuk, T.: Uncertainty quantification for multiscale modeling of polymer nanocomposites with correlated parameters, Composites B, 68, 446–464, https://doi.org/10.1016/j.compositesb.2014.09.008, 2015.

Wang, T., Xue, L., Brimblecombe, P., Lam, Y. F., Li, L., and Zhang, L.: Ozone pollution in China: A review of concentrations, meteorological influences, chemical precursors, and effects, Sci. Total Environ., 575, 1582–1596, https://doi.org/10.1016/j.scitotenv.2016.10.081, 2017.

Wang, Y. and Chen, Y.: Significant Climate Impact of Highly Hygroscopic Atmospheric Aerosols in Delhi, India, Geophys. Res. Lett., 46, 5535–5545, https://doi.org/10.1029/2019gl082339, 2019.

Wang, Y., Li, W., Gao, W., Liu, Z., Tian, S., Shen, R., Ji, D., Wang, S., Wang, L., Tang, G., Song, T., Cheng, M., Wang, G., Gong, Z., Hao, J., and Zhang, Y.: Trends in particulate matter and its chemical compositions in China from 2013–2017, Sci. China Earth Sci., 62, 1857–1871, https://doi.org/10.1007/s11430-018-9373-1, 2019.

WHO: Review of evidence on health aspects of air pollution – REVIHAAP final technical report, World Health Organization, Geneva, 2013.

WHO: Neurological syndrome and congenital anomalies, Zika Situation Report, available at: https://apps.who.int/iris/handle/10665/204348 (last access: 16 December 2019), 1–7, 2016a.

WHO: WHO Global Urban Ambient Air Pollution Database (update 2016), available at: http://www.who.int/airpollution/data/cities-2016/en/ (last access: 8 November 2018), 2016b.

Wiedinmyer, C., Akagi, S. K., Yokelson, R. J., Emmons, L. K., Al-Saadi, J. A., Orlando, J. J., and Soja, A. J.: The Fire INventory from NCAR (FINN): a high resolution global model to estimate the emissions from open burning, Geosci. Model Dev., 4, 625–641, https://doi.org/10.5194/gmd-4-625-2011, 2011.

Wild, O.: Modelling the global tropospheric ozone budget: exploring the variability in current models, Atmos. Chem. Phys., 7, 2643–2660, https://doi.org/10.5194/acp-7-2643-2007, 2007.

Wild, O., Zhu, X., and Prather, M. J.: Fast-J: Accurate Simulation of In- and Below-Cloud Photolysis in Tropospheric Chemical Models, J. Atmos. Chem., 37, 245–282, 2000.

Willmott, C. J., Robeson, S. M., and Matsuura, K.: A refined index of model performance, Int. J. Climatol., 32, 2088–2094, https://doi.org/10.1002/joc.2419, 2012.

Wu, J., Xu, Y., and Zhang, B.: Projection of PM$_{2.5}$ and Ozone Concentration Changes over the Jing-Jin-Ji Region in China, Atmos. Ocean. Sci. Lett., 8, 143–146, 2015.

Xing, J., Wang, S., Zhao, B., Wu, W., Ding, D., Jang, C., Zhu, Y., Chang, X., Wang, J., Zhang, F., and Hao, J.: Quantifying Nonlinear Multiregional Contributions to Ozone and Fine Particles Using an Updated Response Surface Modeling Technique, Environ. Sci. Technol., 51, 11788–11798, https://doi.org/10.1021/acs.est.7b01975, 2017.

Xing, J., Ding, D., Wang, S., Zhao, B., Jang, C., Wu, W., Zhang, F., Zhu, Y., and Hao, J.: Quantification of the enhanced effectiveness of NO$_x$ control from simultaneous reductions of VOC and NH$_3$ for reducing air pollution in the Beijing–Tianjin–Hebei region, China, Atmos. Chem. Phys., 18, 7799–7814, https://doi.org/10.5194/acp-18-7799-2018, 2018.

Zaveri, R. A. and Peters, L. K.: A new lumped structure photochemical mechanism for large-scale applications, J. Geophys. Res., 104, 30387–30415, 1999.

Zaveri, R. A., Easter, R. C., Fast, J. D., and Peters, L. K.: Model for Simulating Aerosol Interactions and Chemistry (MOSAIC), J. Geophys. Res.-Atmos., 113, D13204, https://doi.org/10.1029/2007JD008782, 2008.

Zhao, B., Wu, W., Wang, S., Xing, J., Chang, X., Liou, K. N., Jiang, J. H., Gu, Y., Jang, C., Fu, J. S., Zhu, Y., Wang, J., Lin, Y., and Hao, J.: A modeling study of the nonlinear response of fine particles to air pollutant emissions in the Beijing–Tianjin–Hebei region, Atmos. Chem. Phys., 17, 12031–12050, https://doi.org/10.5194/acp-17-12031-2017, 2017.